Architecture
Image Studies

Vol.7, Issue 1, pp.1339-1352, 2026
DOI: https://doi.org/10.62754/ais.v7i1.1020

https://journals.ap2.pt/index.php/ais/index

Segmentation and visualization of Emphysema lesions through Computed Tomography images

Ragipati Karthik[1], R. Murugan[2], Tripti Goel[3]

Abstract

A large number of individuals in the world suffer from Chronic Obstructive Lung Disease (COPD). There is loss of the lung function in COPD due to emphysema and chronic bronchitis. The early detection of emphysematous lesions is very crucial using Computed Tomography (CT) images. This is intended to improve clinical management and prognosis. In this paper, an automated framework for robust segmentation of emphysema lesions is presented. It also presents morphological features using class specific intensity based thresholding, with morphological operations. The proposed method is based on the percentile-based threshold estimations adopted for each emphysema class. This is to facilitate the different density features and spatial distributions of these classes. The performance is evaluated on a multi-institutional dataset from Indian hospitals located in Chennai, Hyderabad and an online emphysema database. Quantitative analysis reveals distinct differences in the extent and distribution of lesions among the emphysema classes. CLE presents the maximum number of lesions, 61.49 per image and minimum burden (14.31%). PSE has the fewest number of lesions, 35.10 per image but high severity (19.76%). The 3D surface visualization helps to interpret the shape. It presents different intensity patterns and spatial characteristics for each of the emphysema classes. Segmentation and display in combination provide a comprehensive picture of the distribution and degree of emphysema. It serves as a useful tool for clinicians to enhance the diagnosis and determine treatment strategies.

Keywords: *COPD, Emphysema Segmentation, CT, 3D Visualization.*

Introduction

Emphysema is lung disease, one of the forms of COPD. It is a result of damage to the alveoli, or loss of lung tissue elasticity [1]. This causes larger air spaces in the lungs to develop, also leading to reduced exchange of oxygen and maintaining difficulties when breathing [2]. The risk factors for emphysema are long-term cigarette smoking, exposure to environmental and industrial pollutants [3]. The disease of emphysema is considered to be irreversible because lung tissue does not regenerate itself. The aim of the treatment is to alleviate symptoms and decelerate the disease's course [4].

Pulmonary Function Test (PFT) measures patient's Forced Expiratory Volume in 1 second (FEV1) during a forced breath. It is the clinical test to diagnose the severity of COPD. Table 1 shows the COPD severity classification.

Table 1. Severity Classification of COPD

Stage	Classification	Description
I	Mild	FEV_1 greater than or equal to 80% of predicted
II	Moderate	FEV_1 less than 80% and greater than or equal to 50% of predicted
III	Severe	FEV_1 less than 50% and greater than or equal to 30% of predicted
IV	Very Severe	FEV_1 less than 30% of predicted or FEV_1 less than 50% and chronic respiratory failure

[1] Bio-Medical Imaging Laboratory (BIOMIL) National Institute of Technology Silchar, Silchar 788010, Assam, India
[2] Bio-Medical Imaging Laboratory (BIOMIL), National Institute of Technology Silchar, Silchar 788010, Assam, India, Email: murugan.rmn@ece.nits.ac.in, (Corresponding Author)
[3] Bio-Medical Imaging Laboratory (BIOMIL), National Institute of Technology Silchar, Silchar 788010, Assam, India.

According to the decreasing level of FEV_1 in percentages, Global Initiative for Chronic Obstructive Lung Disease (GOLD) stages COPD as mild, moderate, severe and very severe [5]. A schematic illustration of the PFT used in clinical evaluation is shown in Figure 1.

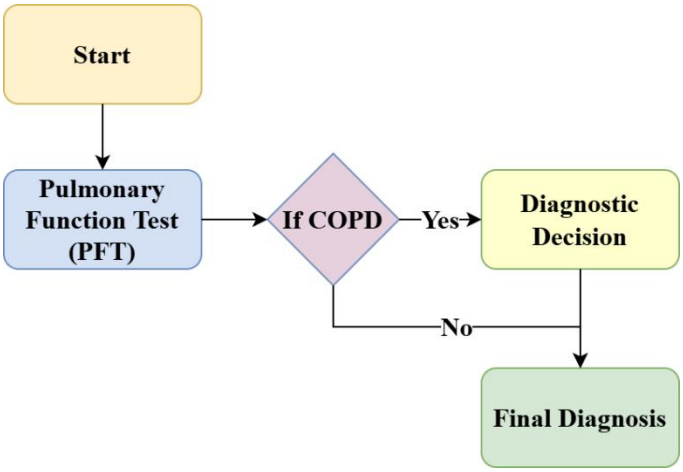

Fig 1. PFT for Diagnosis of COPD

Emphysema commonly manifests in three major categories [6-7]: Centrilobular Emphysema (CLE), Panlobular Emphysema (PLE), and Paraseptal Emphysema (PSE). The anatomical areas impacted, the extent of alveolar damage, and the preponderance of lung zones vary across these groups. For example, PLE causes extensive destruction throughout entire lobules [8], PSE is localized close to the pleural surfaces [9], and CLE mostly affects the central acini of the upper lobes [10]. Figure 2 displays representative CT scans of several kinds of emphysema.

The diagnostic gold standard for emphysema diagnosis is still High-Resolution Computed Tomography (HRCT), however there are difficulties in striking a balance between radiation dosage and image quality [11]. Although Low-Dose CT (LDCT) scanning reduces radiation dangers, it adds noise that makes automated lesion diagnosis more difficult. This study uses deep learning-based segmentation algorithms for precise emphysema localization in CT images in order to overcome these problems. The segmented lesions are then reconstructed using a 3D visualization technique [12]. Emphysema distribution and extent can therefore be easily assessed for a clinical context.

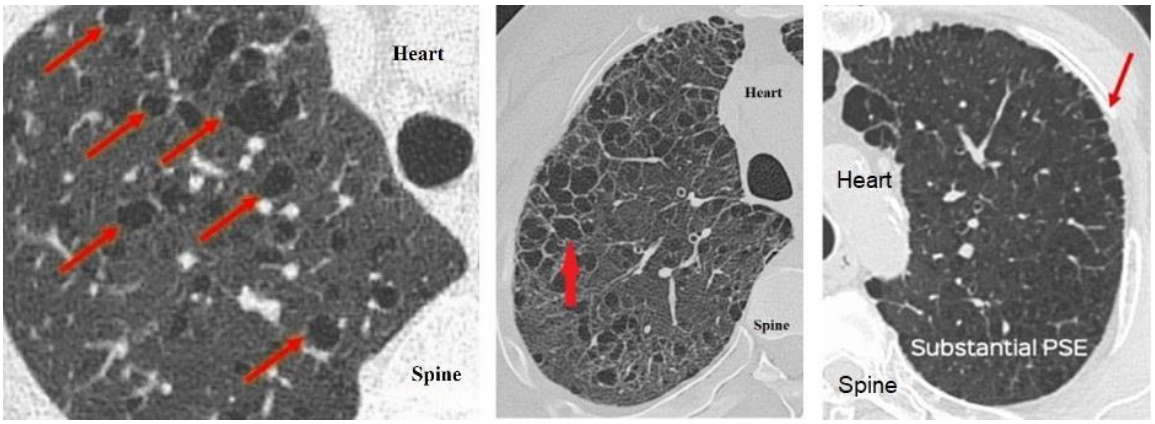

(a) (b) (c)

Fig 2. Emphysema classes observed in CT scans: (a) CLE, (b) PLE, (c) PSE

The contributions of this paper are as follows:

1. The paper presents an automatic computer-aided method for the distinction and classification of classes of emphysematous lesions in human lungs on CT images
2. The study shows combination of emphysema class-specific intensity thresholding with morphological operations to detect the lesions accurately in LDCT and HRCT scans.

3. The proposed method provides 3D visualization of emphysema lesions in the lungs, helping the clinicians understand location and spreading of the lesions and evaluate the disease severity.

The rest of this paper is organized as follows: Section 2 covers the literature survey; Section 3 describes the materials used and proposed methodology; Section 4 presents the experimental results, performance metrics, and comparative evaluations and Section 5 provides the conclusion and future work.

Literature Survey

Deep learning methods recently have improved automated emphysema analysis in CT images. Research in this area can be divided into two main directions: one focuses on lesion segmentation and the other combines segmentation with quantitative analysis and visualization. However, most existing methods have problems, that is, either they do not calculate important lesion metrics or they require too much computing power. This indicates that segmentation methods which can perform well or clearly visualize the 3D image in this aspect are needed.

Emphysema Lesion Segmentation

In the diagnosis and quantification of emphysema, accurate segmentation of emphysematous lesions is important. Sarsembayeva et al. [13] performed the segmentation of COPD lesions using UNet architecture. They obtained good performance in detecting lesion boundaries. But their work was built on a small amount of annotated data. Li et al. [14] focused on segmentation of the lung lobes as a precursor to emphysema quantification. But their technique did not create lesion-level masks. Ramalingam et al. [15] developed an adaptive ResNet combined with Bi-LSTM to detect emphysema. Their model learned features in a sequence, but needed more computing power. Rao et al. [16] introduced Seg-ResUNet. Their model performed well in detecting lesion boundaries. Their approach also employs some of the optimization. However, this approach took a long time to process the images. It is difficult to use in real clinical practice.

Integrated Frameworks and Research Gaps

Wu et al. de [17] provided a full AI pipeline. The presence, stage, and lesion burden of emphysema could be quantified. This demonstrates that end-to-end automatic analysis is feasible. But the pipeline is computationally very expensive. It is difficult to apply in hospitals with limited resources. Vestal et al. [18] used spatial point process modeling to analyze the CT scans. But their method did not have automated segmentation or calculation of quantitative parameters.

Current methods for analyzing emphysema have critical problems that limit their usage in clinical practice. Most existing approaches use only one type of analysis, which cannot combine quantitative lesion measurements with deep learning-based feature recognition very well. Many studies test their methods on a small number of subjects. Thus, the results may not work properly for different types of patients or different CT scanners. Most importantly, the existing research does not focus enough on interactive 3D visualization tools. The clinicians can explore and understand where emphysema is located and how severe it is in the lungs with 3D visualization. These problems indicate that we need new methods that can do all of the following processes together: accurate automated segmentation, calculation of lesion measurements and better 3D visualization. This combination would help clinicians interpret the results better and make better diagnoses.

Materials and Methodology

Data Collection

The primary dataset CT images used in this study were collected from SRM Medical College Hospital & Research Centre in Kattankulathur, Chennai, Tamil Nadu, India [15]. The dataset has 1,000 CT chest images from 40 subjects. The group includes 21 healthy people (14 males, 7 females; average age 35.85 years) and 19 patients with emphysema (17 males, 2 females; average age 66.5 years). The emphysema patients showed different types of emphysema patterns: CLE, PLE, or PSE. The remaining scans revealed normal lung tissue, with about 475 images showing emphysematous lesions. For analysis, 25 sample slices were chosen for each patient.

A secondary dataset comprising 593 CT slices from 193 individuals was obtained from Malla Reddy Narayana Hospital in Hyderabad, Telangana, India. In order to provide a variety of clinical samples for algorithm validation across realistic imaging situations, our cohort included both healthy

persons and patients with one or more emphysema classifications. Examples of emphysema classes from CT scans obtained from Malla Reddy Narayana Hospital in Hyderabad, India, are shown in Figure 3(a).

The third dataset was taken from the Computed Tomography Emphysema Database and included 115 high-resolution CT slices from 39 individuals [19]. Nine nonsmokers, ten smokers without COPD, and twenty smokers with a diagnosis of COPD made up the group. GE LightSpeed QX/i equipment with an in-plane resolution of 0.78 × 0.78 mm, slice thickness of 1.25 mm, tube voltage of 140 kV, and tube current of 200 mAs was used to capture the images. A high-resolution bone algorithm was used for reconstruction. Slices from the upper, middle, and lower lung areas were included in the 512 × 512 pixel images. Different emphysema classes from the Computed Tomography Emphysema Database are shown in Figure 3(b).

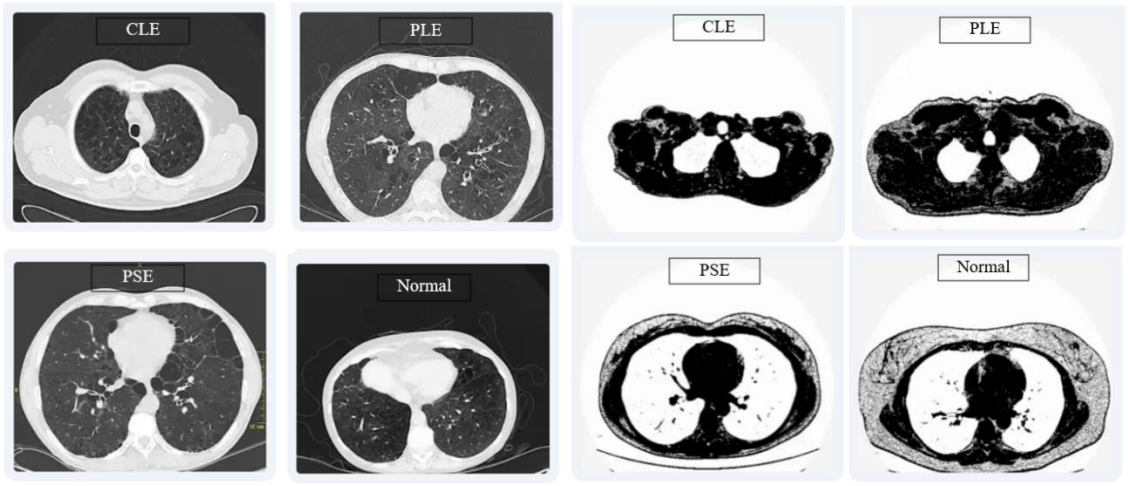

(a) (b)

Fig 3. (a) Malla Reddy Narayana Hospital Database, (b) CT Emphysema Database

Proposed Methodology

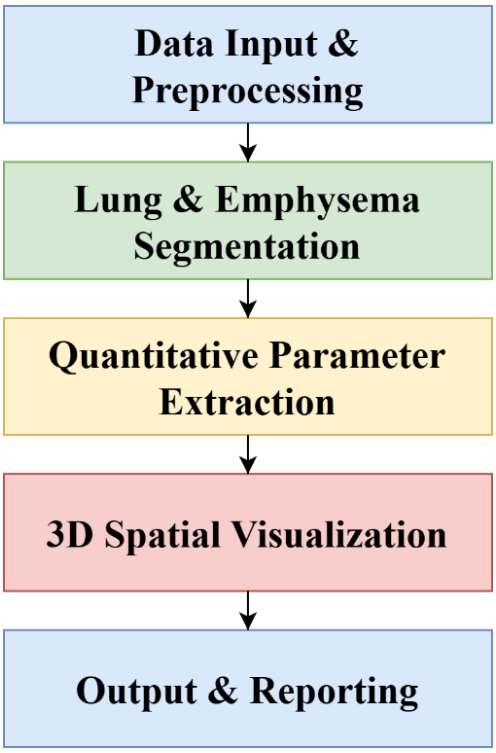

Fig 4. Emphysema Segmentation and 3D Visualization Pipeline

The proposed framework has five main steps (Figure 4) for accurate emphysema lesion detection and interactive spatial analysis. First, CT scan images are loaded and normalized for intensity to keep uniformity across the dataset. Table 2 lists all preprocessing steps used. Pixel values are scaled to [-1, 1] range so lesion detection works well on different CT scanners. Subsequent lung boundaries are identified by automated segmentation. Then, emphysema lesions are identified using class-specific intensity thresholds. CLE, PLE, PSE require different thresholds, due to their density dissimilarities. This thresholding results in binary masks of emphysema regions vs normal lung tissue. Then, morphological techniques including dilation, erosion and closing are performed to enhance the segmentation quality as well as to eliminate noise or artefact.

The clinical metrics are then calculated from the segmented emphysema regions such as number of lesions, total emphysema volume and Low Attenuation Area (LAA) percentage, severity distribution. The segmentations are used to average normalized intensity values contained within segmented lesions as indirect measures of local tissue density. The segmented emphysema luecent areas are next transformed to 3D surface models by applying intensity based elevation mapping. In this step, the intensity range is coupled with each level of emphysema severity. This aids in visual assessment of the shape of lesions and their location relative to the lung anatomy. The 3D representation is fully interactive. The user can rotate the lung to inspect from various directions and study in detail about the emphysema characteristics. The system also generates quantitative lesion reports. It contains segmentation metrics, morphology details and severity values as well as 3D renderings. This allows the clinicians to make a more comprehensive analysis of emphysema when compared with standard 2D CT slices.

Pre-Processing and Lung Segmentation

Table 2. Preprocessing Methods

Step	**Technique**	**Purpose**
Load Image	Computed Tomography (CT)	Raw slice input
Intensity Normalization	Z-score normalization	Remove bias and standardize
Contrast Enhancement	CLAHE (Contrast Limited Adaptive Histogram Equalization)	Enhance lung details
Noise Reduction	Gaussian Blur (3x3, σ=0.5)	Preserve edges, reduce noise
Lung Segmentation	Thresholding + morphological operations	Extract lung regions
Boundary Refinement	Morphological closing	Smooth edges and remove artifacts

Preprocessing of Raw 2D CT Scans The raw 2D CT scans undergo preprocessing pipeline to enhance the image quality and extract lung regions for accurate analysis of emphysema. The process starts by loading each CT slice $I(x, y)$ as a grayscale image. Subsequent step is to perform intensity normalization with Z-score standardization, which can be described as in Eq. (1). This is to reduce intensity bias across the dataset [20].

$$I_z(x, y) = \frac{I(x,y)-\mu}{\sigma} \quad (1)$$

where μ is the lung region's mean and σ is the standard deviation of intensity values.

Min-max scaling was applied to standardize the image intensities [21]. This method rescales the intensity values to fall in between 0 and 255. Equation (2) shows the Min-Max Scaling.

$$I_s(x, y) = 255 \times \frac{I_z(x,y)-\min(I_z)}{\max(I_z)-\min(I_z)} \quad (2)$$

Contrast enhancement using CLAHE helps in improving the visibility of small lung structures and emphysema features [22-23], as shown in Eq. (3).

$$I_{clahe}(x,y) = CLAHE(I_s(x,y)) \tag{3}$$

Gaussian blur filtering reduces noise in the images while saving the important anatomical edges [24-25], as shown in Eq. (4).

$$I_p(x,y) = G_\sigma * I_{clahe}(x,y) \tag{4}$$

where $G_\sigma *$ stands for convolution with Gaussian kernel of standard deviation σ = 0.5.

Automated lung segmentation uses thresholding combined with morphological operations. It isolates and identifies the lung tissue boundaries, as shown in Eq. (5).

$$M(x,y) = \begin{cases} 1, & I_p(x,y) < T \\ 0, & otherwise \end{cases} \tag{5}$$

where T is the intensity threshold value used to identify lung tissue.

Morphological closing further improves the segmentation by smoothing the edges and removing the segmentation artifacts [26], as shown in Eq. (6).

$$M_{closed}(x,y) = (M(x,y) \oplus S) \ominus S \tag{6}$$

where $\oplus$ is the dilation, $\ominus$ denote the erosion and S is the structuring element. This method bridges small gaps and sharp corners in segmentation. It leads to a pair of lung boundaries which are smooth and continuous [27].

This preprocessing streamline ensures that lung tissue is extracted robustly. It offers a strong basement of further research in emphysema lesion detection and quantification.

Qualitative studies of our segmentations, as illustrated in Figure 5, clearly prove that the extracted lung borders are correct. Results show that the automatic masking succeeds. This constitutes a sound basis for the localization and analysis of the emphysema.

(a) (b) (c)

Fig 5. (a) Original CT, (b) Lung Mask, (c) Lung Segmentation Result

Lesion Segmentation

Segmentation of the lesion is a key step in the automated emphysema analysis. It enables us to distinguish and further pinpoint the emphysema regions in CT images [28-29]. The described approach in Fig. 6 utilizes intensity thresholding and morphological operations to search for the lesions in the segmented lung region. This technique utilizes As the emphysema types have differing density properties, multiple threshold values for intensity are applied based on the different emphysema classes. Binary lesion masks are subsequently generated for delineating the diseased tissue from normal lung regions. Subsequently, the morphological closing operations are performed to further refine the delineation and eliminate segmentation artifacts. We can then measure the emphysema burden, with the lesion masks in hand. It encompasses counts of lesions, distributions (i.e. severity distribution) and also spatial arrangement. This then could serve as groundwork for comprehensive clinical characterization. This provides a good trade-off between the computational burden and the

accuracy of the segmentation. This approach allows for analysis of a large number of CT images and retains the clinical relevance. The binary mask of emphysema lesion obtained is seen in Eq. (7).

$$L_{mask}(x,y) = \begin{cases} 1, & I_s(x,y) < T_{class} \text{ and } M_{closed}(x,y) \\ 0, & otherwise \end{cases} \quad (7)$$

where T_{class} is the threshold value used to detect emphysema.

Eq. (8). calculates the percentage of lung area affected by emphysema [30].

$$LAA(\%) = \frac{\sum_{(x,y)\in Lung} L_{mask}(x,y)}{\sum_{(x,y)\in Lung} M_{closed}(x,y)} \times 100 \quad (8)$$

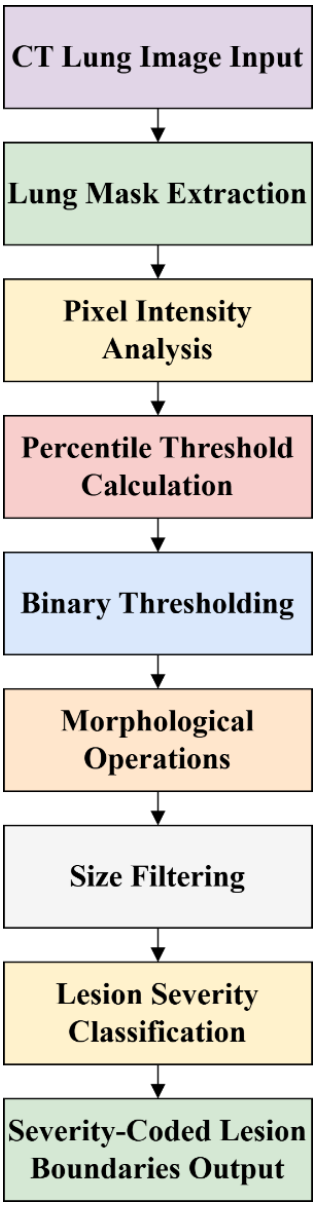

Fig 6. Automated Emphysema Lesion Segmentation Pipeline

Three-Dimensional Visualization of Emphysema Lesions

Plotly and Matplotlib libraries allow viewers to generate 3D surface images of the emphysema lesions detected in the segmentation phase. The heights of the 3D surface are determined according to the pixels intensity. This technique gives more depth than seeing CT slices alone. By using interactive tools, clinicians are able to manipulate the 3D model so as to rotate it and look at the lesions

from various angles which reveal their shape, the severity declared through colour coding as well as how they spread in different segments of the lungs.

The main advantage of this method is that it illustrates the correlation between emphysema lesions and surrounding lung anatomy. It aids in the comprehension of general distribution pattern of emphysema disease in the lungs by radiologists. The screen provides clear images for clinical findings. The lesions can be examined in detail by clinicians with facilities such as interactive rotation and zoom.

Results

The emphysema lesion segmentation and visualization were implemented in Google Colab using a Tesla T4 GPU, and Python 3.10 with TensorFlow 2.15. This setup allowed us to process many CT images efficiently. The emphysema regions detected from CT scans were sorted into four groups namely CLE, PLE, PSE and normal lung tissue. All steps of the work were carried out in a full pipeline from preprocessing the images, segmenting the lungs, finding lesions and creating 3D views. All these steps were done on this cloud platform. This made it easy to test the method on different datasets and get the results.

Lesion Segmentation Results

The lesion segmentation module was built using Python with OpenCV for processing the images, NumPy for doing calculations and scikit-image for morphological operations. Different threshold values are used for each class of emphysema because they show different density levels in the images. Binary masks were made to mark where the emphysema is in the lung tissue. Then the edges of the lesions were found using contour detection methods.

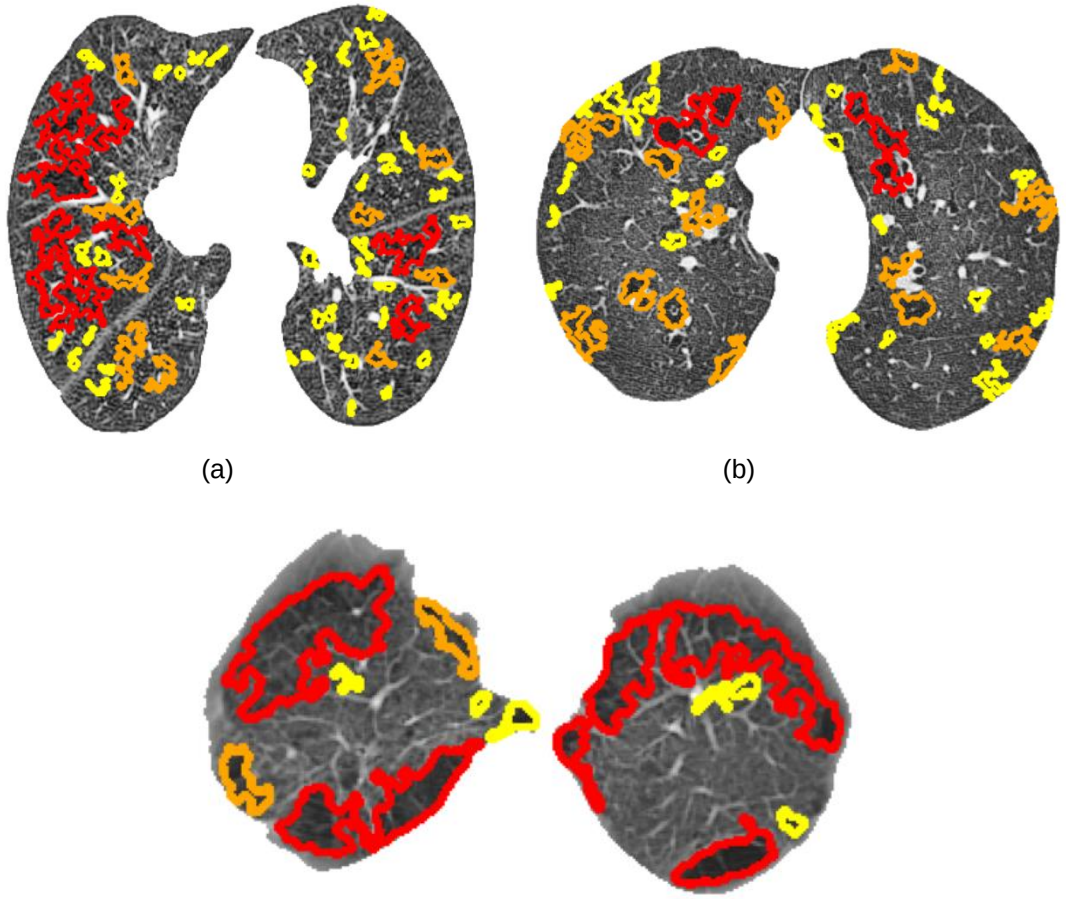

(a) (b)

(c)

Fig 7. Quantified Lesion Boundaries for Emphysema Classes: (a) CLE, (b) PLE, (c) PSE

Each lesion was classified by how severe it was. It is shown with different-coloured boundaries: red for severe lesions, orange for moderate ones, and yellow for mild ones. Using different colours makes it easier for clinicians to understand where the lesions are and how serious they are. Figure 7 shows the severity-coloured lesion boundaries for CLE, PLE and PSE. Figure 8 shows corresponding binary lesion masks, which confirm that the emphysema areas are located correctly across all emphysema classes.

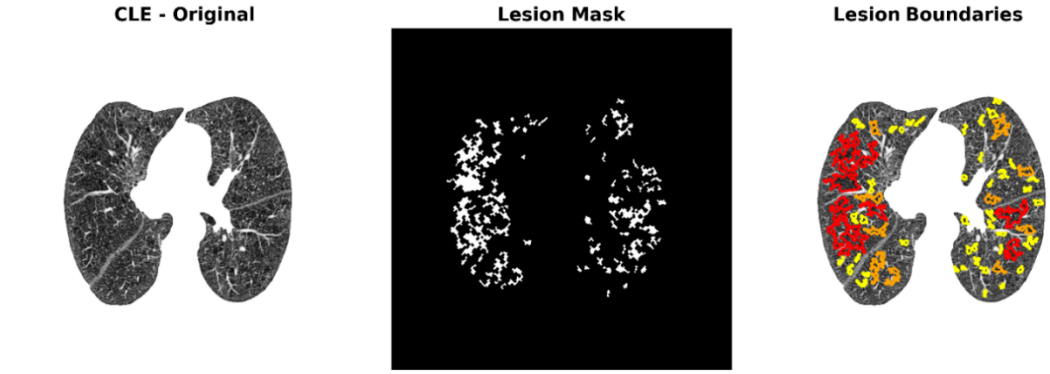

(a)

(b)

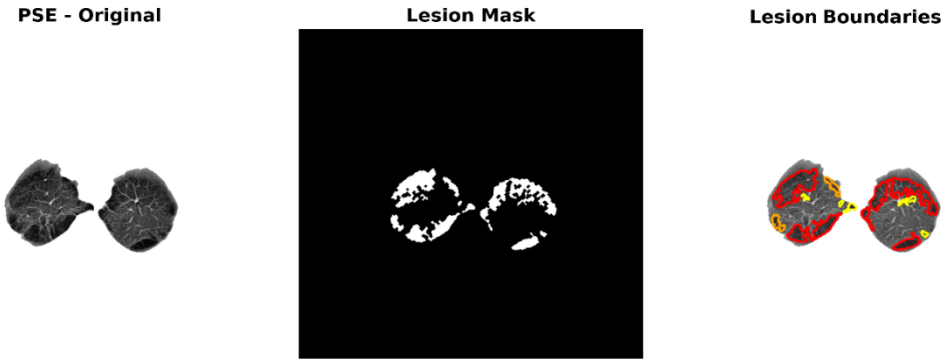

(c)

Fig 8. Quantified Lesion Segmentation for Emphysema Classes: (a) CLE, (b) PLE, (c) PSE

Performance Analysis on Lesions

Emphysema lesions were measured and analyzed for all three emphysema classes using detailed severity classification. Table 3 shows how many lesions were found at each severity level (mild, moderate, severe) and the total emphysema burden for each class.

Table 3. Emphysema Lesion Delineation

Class	Mild (%)	Moderate (%)	Severe (%)	Combined (%)
CLE	76.85	15.80	7.35	14.31
PLE	71.71	18.64	9.66	15.64
PSE	66.65	18.40	14.95	19.76

The three emphysema classes showed different patterns of the damage. For CLE, most of the lesions were mild, and only a small portion were severe. The disease seems more limited and mainly around the small airways. In PLE, there were again many mild lesions, but the share of moderate lesions was higher. This suggests that the damage is spread more widely in the lung tissue. In the case of PSE, we observed highest proportion of severe lesions among the three classes. This is consistent with the typical paraseptal pattern in which the lung periphery is predominantly involved. Through these observations, we can see that our segmentation technique is capable of distinguishing among the three emphysema classes and provide a quantitative measure for how severe the disease is in different parts of the lung.

Lesion Burden Analysis and Disease Progression Patterns

Image based lesion quantification in this work reveals that disease burden pattern is unique for each emphysema class, while lesion shape and size also vary with severity. The average number of lesions per image and the average size of lesions are recorded for all three emphysema types, mild, moderate, and severe for each class in Table 4.

Table 4. Lesion Burden and Morphology Across Emphysema Classes

Class	Avg Lesions/Image	Severe Lesion Size (px)	Moderate Lesion Size (px)	Mild Lesion Size (px)
CLE	61.49	385	185	42
PLE	39.43	520	215	48
PSE	35.1	445	190	45

CLE showed the greatest number of lesions on an image basis (61.49 lesions/image). This illustrates the undue destruction common for this nature. PLE had moderate lesion count (39.43 lesions/image). Though some (less) severe lesions were very large (520 pixels), implying that they have for the same number reduced but bigger damaged area of the tissue. PSE showed the lowest lesion number (35.10 lesions/image), with a large percentage of severe ones too (445 pixels). This corresponds to the focal damage distribution in paraseptal emphysema. Severe lesions were 8-11 times larger than mild ones for all classes. These numbers demonstrate a distinct pattern for each emphysema class and confirm that our segmentation method is effective in counting lesions and measuring their shape and size.

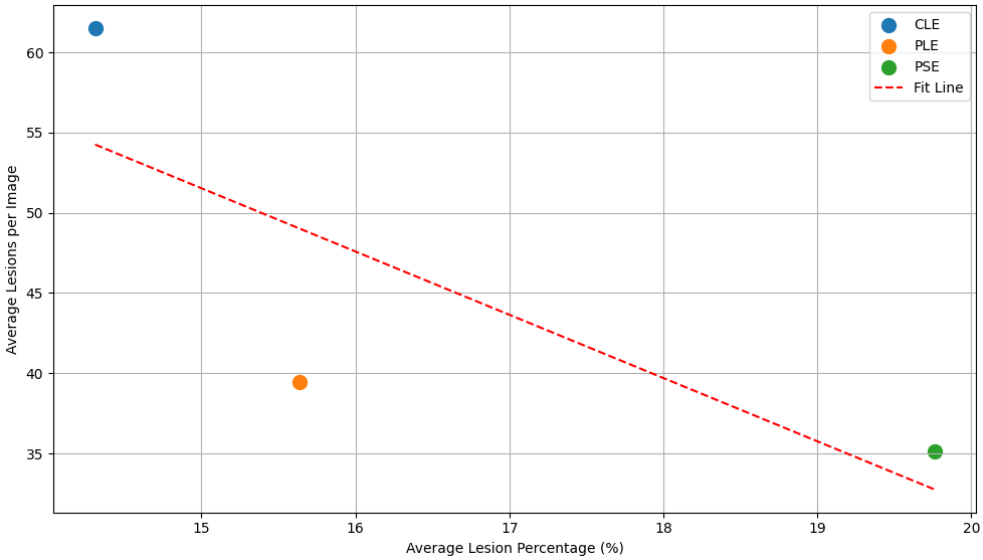

Fig 9. Correlation Between Lesion Percentage and Lesion Count

From the scatter plot in Figure 9, lesion burden percentage and lesion count are inversely related among the emphysema classes. CLE has the moderate emphysema rate (14.31%) however, the highest lesion amounts (61.49 lesions per image). It contains numerous randomly distrbuted little lesions. PSE is the most loaded (19.76%) and places the smallest number of lesions (35.10 lesions), which are therefore larger, clustered ones as expected from paraseptal damage. PLE is a compromise of these two. This inverse relationship demonstrates that a complete evaluation of the disease require both number and burden measurement, this also indicates characteristic patterns for each emphysema class.

Three-Dimensional Spatial Visualization of Emphysema Lesions

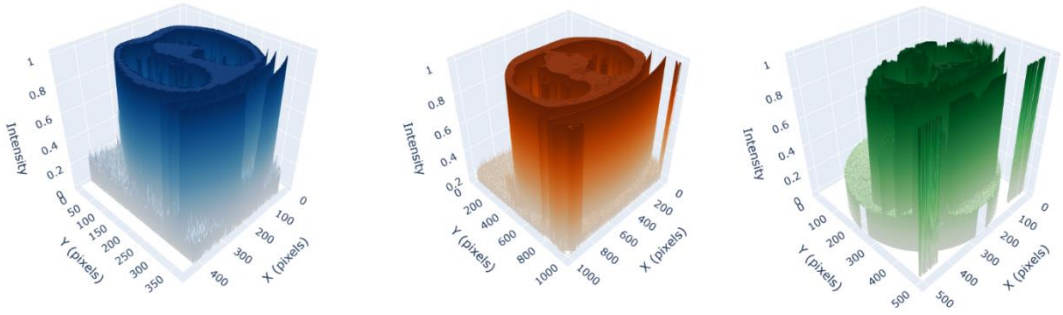

(a) (b) (c)

Fig 10. 3D Surface Comparison of Emphysema : (a) CLE, (b) PLE, (c) PSE

3D visualization helps us to better understand how emphysema lesions are arranged and shaped in different disease classes. Figure 10 shows the volumetric intensity profiles for example CT slices of CLE, PLE and PSE as elevation maps where the surface height matches the pixel intensity. This approach shows distinct lesion patterns. CLE has a more diffuse and fine texture. PLE has focal high-intensity areas more apparent. PSE presents focal hyperattenuated images, characteristic of paraseptal lesions.

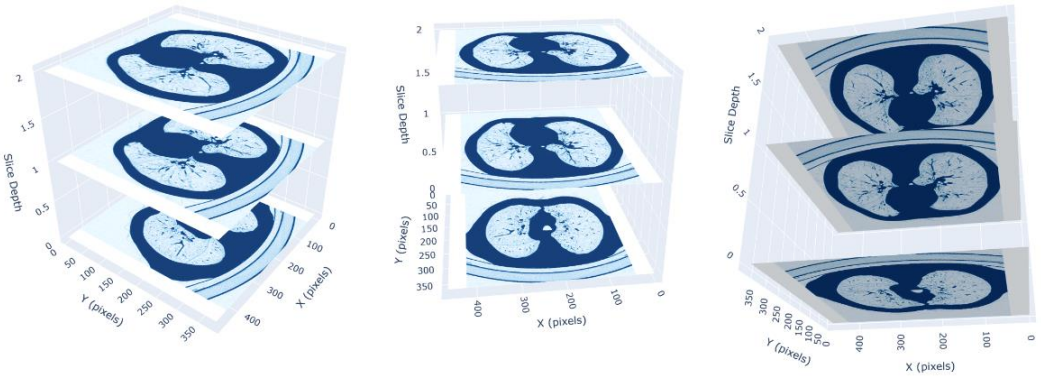

Fig 11. Spatial Distribution in CLE - Stacked Slice Analysis

Figure 11 demonstrates a stacked 3D reconstruction of sequential CLE slices in top, mid and bottom lung regions in another patient case. This enables image analysis of emphysema morphology as a function of anatomy depth. "Layers" demonstrates variation levels and that the disease progresses spatially in the cranio-caudal direction. This provides full anatomical context, thereby facilitating a better comprehension of the disease distribution patterns and demonstrates that our method has the ability to do phenotyping.

Conclusion and Future work

In this study, we propose an automated approach for the segmentation and characterization of emphysema lesions based on class-specific intensity thresholding in combination with 3D visualization. The method works well for finding emphysema classes with distinct morphology differences. From the quantitative results, CLE with the highest number of lesions per image (61.49) presents the lowest severity burden (14.31%), while PSE with the least number of lesion count (35.10), has highest burden (19.76%). Using Plotly and Matplotlib with intensity-based segmentation gives better spatial understanding than normal 2D slice viewing. This helps clinicians in better emphysema diagnosis and management.

Future work involves extending the framework for full 3D CT datasets in order to analyze complete lung volumes. Machine learning techniques will be used to automatically set threshold values better for different scanners. Automatic classification of emphysema phenotypes is also planned to improve diagnosis accuracy. For clinical use, multi-hospital validation and integration with hospital systems for real-time work are needed. Augmented reality visualization and disease progression models will help clinicians manage emphysema patients better.

Author Contributions

For the creation of the current paper, each author made an equal contribution.

Funding

The authors affirm that this manuscript was not prepared with the help of any money, grants, or other resources.

Data Availability Statement

The datasets generated during the current study are available from the corresponding author by reasonable request.

Declarations

Conflict of interest

There are no competing interests, according to the authors.

Ethical Approval

None of the authors of this article have conducted any experiments using humans or animals.

References

[1] Sørensen L, Shaker SB, de Bruijne M (2010) Quantitative analysis of pulmonary emphysema using local binary patterns. IEEE Trans. Med. Imaging 29(2):559–569.

[2] T. Fitzmaurice et al., "Defining CT subtypes in chronic obstructive pulmonary disease: Real world daily practice does not meet guidelines," Curr. Probl. Diagn. Radiol., Jul. 2025, doi: 10.1067/j.cpradiol.2025.07.001.

[3] X. Wang, W. Hu, and J. Zhang, "Advances in pathophysiology and assessment methods of chronic obstructive pulmonary disease with frailty," Chin. Med. J. Pulm. Crit. Care Med., Feb. 2025, doi: 10.1016/j.pccm.2025.02.002.

[4] Lidén M, Hjelmgren O, Vikgren J, Thunberg P (2020) Multi-reader-multi-split annotation of emphysema in computed tomography. J. Digit. Imaging 33(5):1185–1193.

[5] P.S. Hiremath, P.M. Bannigidad, Classification of chronic obstructive pulmonary disease in computed tomography images using deep learning models, Biomed. Signal Process. Control 68 (2021) 102717.

[6] Mondal S, Sadhu AK, Dutta PK (2021) Automated diagnosis of pulmonary emphysema using multi-objective binary thresholding and hybrid classification. Biomed. Signal Process. Control.

[7] M. Damiani Ferretti, M. R. Rimondi, and M. Zompatori, "An unusual association of emphysema and interstitial disease," J. Med. Imag. Intervent. Radiol., vol. 12, Art. no. 1, Jan. 2025, doi: 10.1007/s44326-024-00047-6.

[8] Zhou X, Yang X, Shen D (2019) Edge detection for medical image segmentation using a hybrid model. J. Med. Imag. 6(2):021008. https://doi.org/10.1117/1.JMI.6.2.021008

[9] Wu Y., Xia S., Liang Z., et al. Artificial intelligence in COPD CT images: identification, staging, and quantitation. Respir Res. 2024;25:319. https://doi.org/10.1186/s12931-024-02913-z

[10] Kumari S, Mittal N (2022) Comparative analysis of noise reduction filters for medical images. In: Proc. Int. Conf. Computing, Communication, Intelligent Syst. (ICCCIS), pp 1–6. https://doi.org/10.1109/ICCCIS10469449

[11] Isaac A, Nehemiah HK, Isaac A, Kannan A (2020) Computer-aided diagnosis system for diagnosis of pulmonary emphysema using bio-inspired algorithms. Comput. Biol. Med. 124:103940. https://doi.org/10.1016/j.compbiomed.2020.103940

[12] Xie W, Jacobs C, Charbonnier J-P, Slebos DJ, van Ginneken B (2023) Emphysema subtyping on thoracic computed tomography scans using deep neural networks. Sci. Rep.

[13] Sarsembayeva T, et al. (2022) UNet model for segmentation of COPD lung lesions on computed tomography images. In: Proc. 7th Int. Conf. Digit. Technol. Educ., Science, Industry (DTESI), Almaty, Kazakhstan, Oct 20–21.

[14] Li TZ, et al. (2021) Quantifying emphysema in lung screening computed tomography with robust automated lobe segmentation. J. Med. Imaging.

[15] Ramalingam R, Chinnaiyan V (2024) Intelligent optimization-based pulmonary emphysema detection with adaptive multi-scale dilation assisted residual network with Bi-LSTM layer. Biomed. Signal Process. Control 88:105643. https://doi.org/10.1016/j.bspc.2023.105643

[16] Rao KBV Brahma, et al. (2025) A novel pulmonary emphysema detection using Seg-ResUnet-based abnormality segmentation and enhanced heuristic algorithm-aided deep learning. Expert Syst. Appl. 268:126250

[17] Wu Y, Xia S, Liang Z, Chen R, Qi S (2024) Artificial intelligence in COPD CT images: identification, staging, and quantitation. Respir. Res. 25:319. https://doi.org/10.1186/s12931-024-02913-z

[18] Vestal BE, et al. (2022) Using a spatial point process framework to characterize lung computed tomography scans. Spatial Stat.

[19] Sørensen L (2022) Emphysema Database. https://lauge-soerensen.github.io/emphysema-database/.

[20] Sadia RT, Ahmad A, Malik AS, Abdullah MF (2024) CT image denoising methods for image quality improvement: A comprehensive review. Front. Public Health 12:1340572. https://doi.org/10.3389/fpubh.2024.1340572.

[21] Y. Wang et al., "Whole-lung CT radiomic nomogram for the identification of chronic obstructive pulmonary disease," Mil. Med. Res., vol. 11, no. 1, Art. no. 29, May 2024, doi: 10.1186/s40779-024-00516-9.

[22] Dimitrovski I, et al. (2024) U-Net ensemble for enhanced semantic segmentation in remote sensing imagery. Remote Sens. 16(12):2077. https://doi.org/10.3390/rs16122077.

[23] F. Alafer et al., "A Comprehensive Exploration of L-UNet Approach: Revolutionizing Medical Image Segmentation," IEEE Access, early access, Oct. 2024, doi: 10.1109/ACCESS.2024.3413038.

[24] Wang H, Chen Y, Li Z, Zhang Q (2024) Expanding horizons: U-Net enhancements for semantic segmentation in oceanic remote sensing. J. Remote Sens. 2024:0196. https://doi.org/10.34133/remotesensing.0196.

[25] A. Yadav et al., "A comparative analysis of image harmonization techniques in mitigating differences in CT acquisition and reconstruction," Phys. Med. Biol., vol. 70, no. 5, Art. no. 055015, Feb. 2025, doi: 10.1088/1361-6560/adabad.

[26] Ullah F, Noor A, Ahmad S, et al. (2025) A new hybrid image denoising algorithm using adaptive median filter and modified decision-based median filter for medical imaging applications. Sci. Rep. 15:1847. https://doi.org/10.1038/s41598-025-92283-3.

[27] M. A. Reyes-Aldasoro et al., "Sparse keypoint-based fissure segmentation using geometric deep learning," Int. J. Comput. Assist. Radiol. Surg., vol. 19, no. 10, pp. 1–12, Oct. 2024, doi: 10.1007/s11548-024-03310-z.

[28] Schwarzhans F, Geier B, Pötsch N, et al. (2025) Image normalization techniques and their effect on the robustness and predictive power of breast MRI radiomics. Eur. J. Radiol. 182:111726. https://doi.org/10.1016/j.ejrad.2024.111726.

[29] T. Zhou et al., "A clinical-radiomics nomogram based on automated segmentation of chest CT to discriminate PRISm and COPD patients," Eur. J. Radiol. Open, vol. 13, Art. no. 100580, 2024, doi: 10.1016/j.ejro.2024.100580.

[30] Y. Yin, E. A. Hoffman, and C. L. Lin, “Lung lobar segmentation in emphysema: A novel framework based on anatomical and physiological features,” Med. Phys., vol. 43, no. 8, pp. 4565–4576, Aug. 2016, doi: 10.1118/1.4956781.